

Transition Metal–Boron Complexes B_nM : From Bowls ($n = 8–14$) to Tires ($n = 14$)*

SI-DIAN LI,^{1,2} CHANG-QING MIAO,² JIN-CHANG GUO,² GUANG-MING REN²

¹*Institute of Molecular Science, Shanxi University,
Taiyuan 030006, Shanxi, People's Republic of China*

²*Institute of Materials Science and Department of Chemistry, Xinzhou Teachers' University,
Xinzhou 034000, Shanxi, People's Republic of China*

Received 21 February 2006; Revised 20 April 2006; Accepted 21 April 2006

DOI 10.1002/jcc.20497

Published online 18 September 2006 in Wiley InterScience (www.interscience.wiley.com).

Abstract: Transition metal–boron complexes B_nM have been predicted at density functional theory level to be molecular bowls ($n = 8–14$) hosting a transition metal atom (M) inside or molecular tires ($n = 14$) centered with a transition metal atom. Small B_n clusters prove to be effective inorganic ligands to all the VB–VIII B transition metal elements in the periodic table. Density functional evidences obtained in this work strongly suggest that bowl-shaped fullerene analogues of B_n units exist in small B_nM complexes and the bowl-to-tire structural transition occur to the first-row transition metal complexes B_nM ($M = Mn, Fe, Co$) at $n = 14$, a size obviously smaller than $n = 20$ where the 2D–3D structural transition occurs to bare B_n . The half-sandwich-type $B_{12}Cr$ (C_{3v}), full sandwich-type $(B_{12})_2Cr$ (D_{3d}), bowl-shaped $B_{14}Fe$ (C_2), and tire-shaped $B_{14}Fe$ (D_{7d}) and $B_{14}Fe^-$ (C_{7v}) are the most interesting prototypes to be targeted in future experiments. These B_nM complexes may serve as building blocks to form extended boron-rich B_nM_m tubes or cages ($m \geq 2$) or as structural units to be placed inside carbon nanotubes with suitable diameters.

© 2006 Wiley Periodicals, Inc. J Comput Chem 27: 1858–1865, 2006

Key words: transition metal–boron complexes; density functional theory; structures; stabilities; IR spectra; structural transition

Introduction

In stark contrast with the three-dimensional structural units (like icosahedral B_{12} and octahedral B_6) that dominate boron chemistry, small boron neutrals B_n and anions B_n^- ($n = 3–15$) have been confirmed to possess planar or quasi-planar geometries in recent photoelectron spectroscopy and density functional theory (DFT) investigations.^{1–7} The planarity of B_n clusters originates from their multiple aromaticity (σ and π) and antiaromaticity in molecular orbital (MO) theory and the 2D–3D structural transition occurs to bare B_n at tubular B_{20} .⁸ The aromaticity of planar boron clusters was also confirmed in terms of topological resonance energies even when multicyclic boron clusters had $4n$ π -electrons, in conflict with the well-established Huckel rule of aromaticity.⁹ Small B_n have also been predicted to be a new class of inorganic ligands, as demonstrated in the cases of LiB_8^- (C_{7v}),² B_6A (C_{6v}) ($A = Be, Mg, Ca, Sr$),¹⁰ and B_7A (C_{7v}) ($A = Li, Na, K, Rb, Cs$).¹¹ In these systems, however, the A– B_n interactions are basically ionic. In a recent communication,¹² our group proposed a new class of sandwich-type complexes $(B_nX)_2M$ ($n = 6, 7$; $X = B, C, N$; $M = Mn, Fe, Co, Ni$), in which the transition metal center M is directly coordinated to two parallel $[B_6C]^{2-}$ or $[B_7B]^{2-}$ ligands.¹³ In this work, we explore the

possibility at DFT level to form transition metal–boron complexes B_nM with bigger B_n ligands in the size range of $n = 8–14$. The DFT structures of B_nM complexes turned out to be molecular bowls hosting a transition metal atom inside ($n = 8–14$) or molecular tires centered with a transition metal atom ($n = 14$), with M including all the VB–VIII B elements in the periodical table. DFT evidences obtained in this work strongly suggest that bowl-shaped fullerene analogues of B_n units exist in small B_nM ($n = 8–14$) and the bowl-to-tire structural transition occurs to the first-row transition metal complexes B_nM ($M = Mn, Fe, Co$) at $n = 14$, a size obviously smaller than $n = 20$ where the 2D–3D structural transition occurs to bare B_n , as mentioned earlier. The half-sandwich-type $B_{12}Cr$ (C_{3v}), full sandwich-type $(B_{12})_2Cr$ (D_{3d}), bowl-shaped $B_{14}Fe$ (C_2), and tire-shaped $B_{14}Fe$ (D_{7d}) and $B_{14}Fe^-$ (C_{7v}) with the approximate diameter of 3.8 Å are the most interesting prototypes to be targeted in future experiments. These complex units may

Correspondence to: S.-D. Li; e-mail: lisidian@yahoo.com

Contract/grant sponsor: Natural Science Foundation of China; contract/grant number: 20573088

Contract/grant sponsor: Shanxi Natural Science Foundation; contract/grant number: 20021029

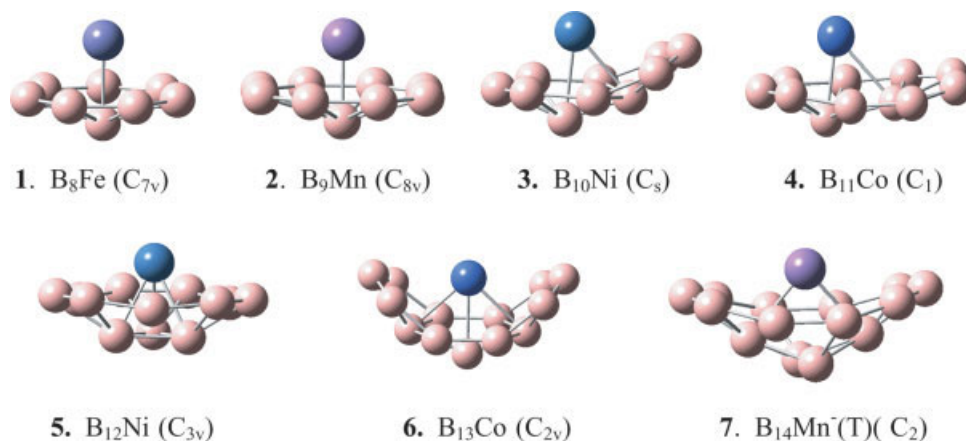


Figure 1. Bowl-shaped B_nM ($n = 8–14$) at B3LYP/6–311 + G(3 df). [Color figure can be viewed in the online issue, which is available at www.interscience.wiley.com]

serve as building blocks to form extended boron-rich B_nM_m tubes or cages with multiple transition metal centers ($m \geq 2$) or as structural units to be placed inside carbon nanotubes in suitable sizes, which may find important applications in both chemistry and materials science. To the best of our knowledge, there has been no investigation reported to date on bowl- or tire-shaped transition metal–boron B_nM complexes.

Computational Procedure

Initial structural optimizations, frequency analyses, and natural bonding orbital (NBO) analyses were performed with the hybrid DFT-B3LYP method¹⁴ with the basis of 6-31+G(d) for B and Li and Lanl2dz for transition metal centers (Lanl2dz contains a Los Alamos effective core potential for transition metals¹⁵ and the combined basis will be denoted as 6-31+G(d)/Lanl2dz hereafter). The second-order Møller–Plesset perturbation procedure (MP2/6-31+G(d)/Lanl2dz) produced essentially the same structures as DFT with slightly different bond lengths (within 4%). The optimized structures were finally refined at DFT-B3LYP with a bigger basis of 6-311+G(3df) and the obtained results proved to be quite insensitive to the bases employed. Based

upon this observation, the B3LYP/6-31+G(d)/Lanl2dz results obtained for double-tire sandwich-type complexes and for systems containing the second- or third-row transition metals are directly used in this work without further optimizations. The widely used nucleus-independent chemical shifts (NICS)¹⁶ were calculated for ghost atoms located 1.0 Å above the B₇-ring centers (NICS¹) to assess the ring current effect of the systems. Figure 1 depicts the optimized bowl-shaped structures of B_nM ($n = 8–14$), Figure 2 shows the optimized structures of half-sandwich-type $B_{12}Cr$ and full sandwich-type $(B_{12})_2Cr$ compared with the slightly off-planed B_{12} ligand (C_{3v}), and Figure 3 demonstrates the relative stabilities of the low-lying isomers of $B_{12}C\bar{o}$ (a), $B_{14}Fe$ (b), and $B_{14}Fe^-$ (c). The calculated infrared (IR) spectra of tire-shaped $B_{14}Fe$ (D_{7d}), $B_{14}Fe$ (C_{7v}), and $B_{14}Fe^-$ (C_{7v}) are compared with that of bowl-shaped $B_{14}Fe$ (C_2) in Figure 4 and the geometrical and electronic properties of high symmetry tire-shaped structures (D_{7d} or C_{7v}) summarized in Table 1. The tire-shaped geometries of $B_{14}M$, their Li^+ -containing complexes, and double-tire sandwich-type $[B_{14}M]_2M'$ are exhibited in Figure 5. Figure 6 shows the MO pictures of the prototypic tire-shaped complex $B_{14}Fe^-$ involving the partially filled Fe 3d orbitals and interligand interactions between B₇ ligands. Triplet (T) and doublet (D) states are labeled in parentheses

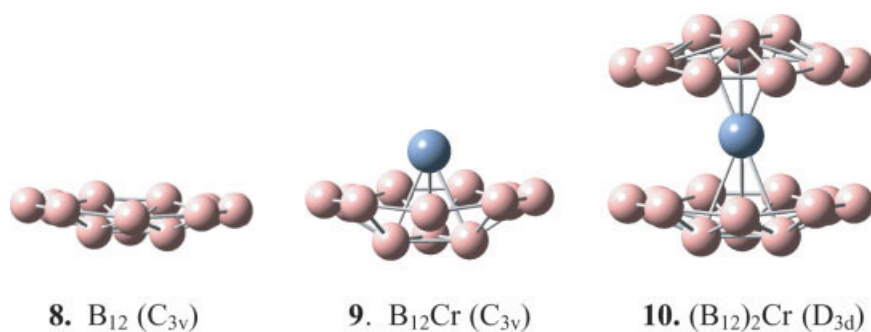


Figure 2. Half-sandwich-type $B_{12}Cr$ (C_{3v}) and full sandwich-type $(B_{12})_2Cr$ (D_{3d}) compared with B_{12} ligand (C_{3v}) at B3LYP/6–311 + G(3df). [Color figure can be viewed in the online issue, which is available at www.interscience.wiley.com]

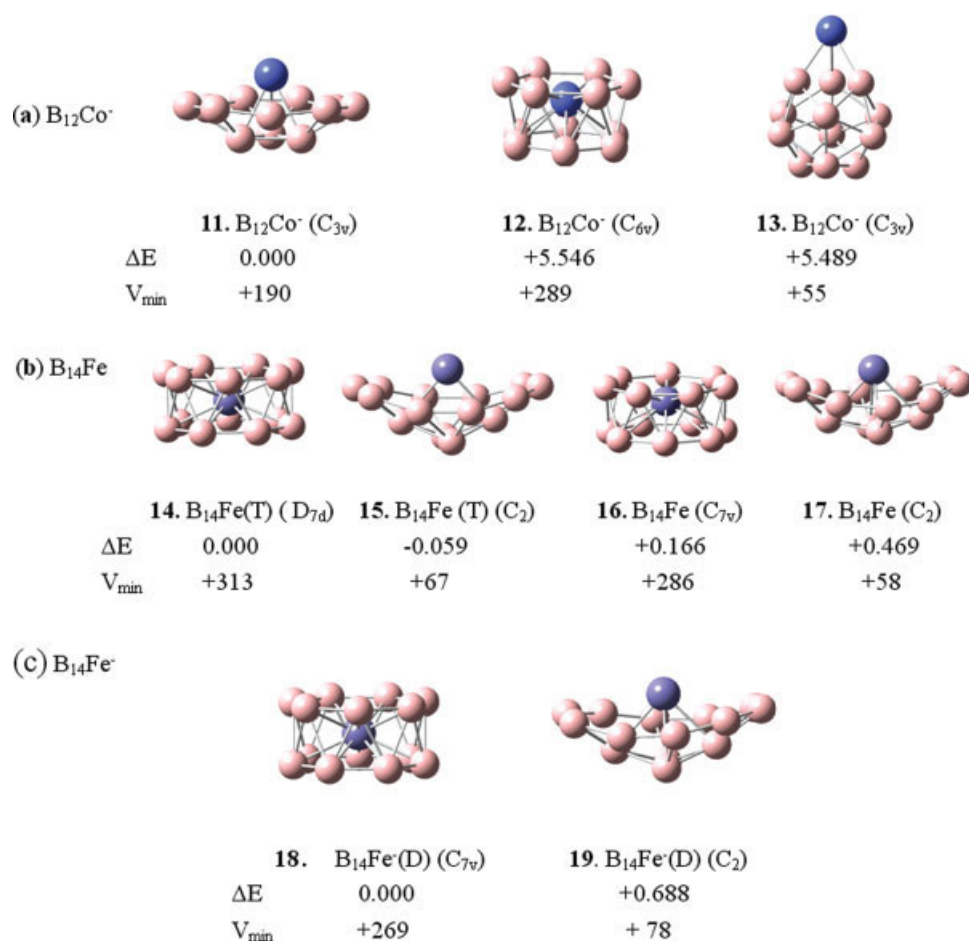


Figure 3. Relative energies ($\Delta E/eV$) and the lowest vibrational frequencies (ν_{min}/cm^{-1}) of the low-lying isomers of $B_{12}Co^-$ (a), $B_{14}Fe$ (b), and $B_{14}Fe^-$ (c) at B3LYP/6-311 + G(3df). [Color figure can be viewed in the online issue, which is available at www.interscience.wiley.com]

throughout Figures 1–5 and Table 1 while all the other structures correspond to singlet (S) states. Detailed results obtained for 106 B_nM complexes are collectively presented in Supporting Information. As small B_n and B_n^- have all been confirmed to exist as planar or quasi-planar species in gas phases,^{1–7} it is reasonable to expect that their bowl-shaped complexes B_nM (see Fig. 1), which can be systematically obtained by coordinating a transition metal atom M from one side along the molecular axis of B_n ligands ($n = 8–14$) without destroying the basic atomic connectivity, be stable species detectable in gaseous phases. As ligand sizes increase, the stress caused by the increased curvature of the ligands increases in bowl-shaped structures. When the number of boron atoms reaches 14, two tire-shaped $B_{14}Fe$ structures are found to be very close in energies with their bowl-shaped isomers, while for $B_{14}Fe^-$ monoanions, the tire-shaped structure is clearly favored by about 0.688 eV over its bowl-shaped isomer, indicating a bowl-to-tire structural transition at $n = 14$. These optimized geometries are well maintained when symmetry constraints are totally released during structural optimizations and their wavefunctions confirmed to be stable. Extensive searches produced no structures with lower energies than the results reported in this

work. All the calculations in this work were performed using the Gaussian 03 program.¹⁷

Results and Discussion

B_nM Molecular Bowls ($n = 8–14$)

Both the B-centered planar $B_8^{2-} (D_{7h})$ and $B_9^- (D_{8h})$ with 6π -electrons^{1,2} are distorted to form shallow bowl-shaped B_n ligands when incorporated in 12-electron $B_8Fe (C_{7v}, \mathbf{1})$ and $B_9Mn (C_{8v}, \mathbf{2})$, with the central B atoms pushed out of the B_7 or B_8 planes by ~ 0.60 Å. Similar bowl-shaped structures have been obtained for two 12-electron complex series with the formula of B_8M and B_9M , respectively, with M including all the VIB–VIII B transition metals (except B_9Cr^- which is distorted to a C_s structure, see Supporting Information for details). The quasi-planar $B_{10} (C_{2h})$ and $B_{12} (C_{3v}, \mathbf{8})$ neutrals, both of which also have 6π electrons,⁷ are severely distorted to form 16-electron bowl-shaped $B_{10}Ni (C_s, \mathbf{3})$ and $B_{12}Ni (C_{3v}, \mathbf{5})$, in which the Ni centers can be replaced with Co, Rh, Pd, Ir, or Pt to form two 16-electron complex series with the formula of $B_{10}M$ and

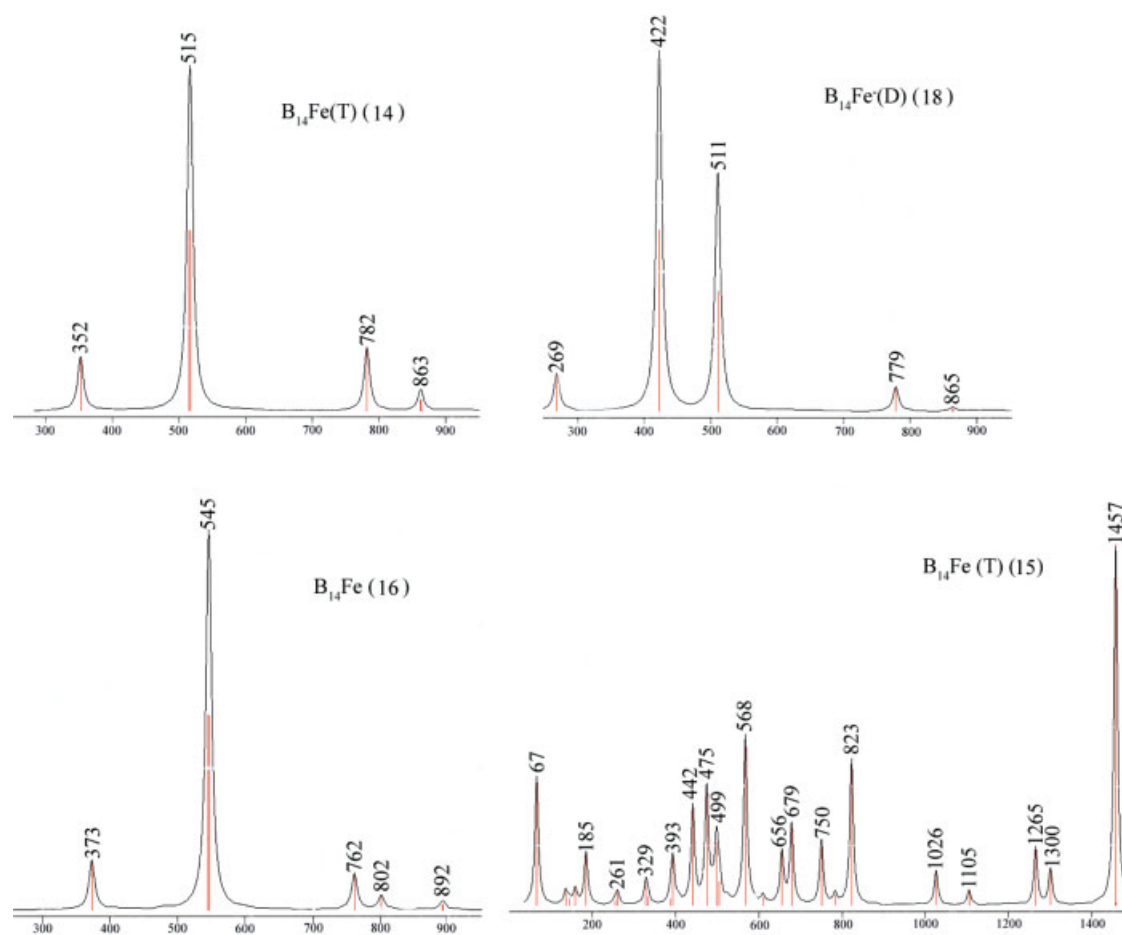


Figure 4. Comparison of the calculated IR spectra (in cm^{-1}) of the tire-shaped $B_{14}\text{Fe}$ (D_{7d} , 14), $B_{14}\text{Fe}$ (C_{7v} , 16), and $B_{14}\text{Fe}^-$ (C_{7v} , 18) and that of the bowl-shaped $B_{14}\text{Fe}$ (C_{2v} , 15) at B3LYP/6-311 + G(3df). [Color figure can be viewed in the online issue, which is available at www.interscience.wiley.com]

$B_{12}M$, respectively. Each $B_{12}M$ (C_{3v}) possesses three B atoms at its bottom that are pushed out of the quasi-plane of the nine peripheral B atoms by $\sim 0.9 \text{ \AA}$ as a result of the asymmetrical coordination of the transition metal center M from the opposite

side. More interestingly, a B_{12} ligand (C_{3v} , **8**) can be employed to form the 12-electron half-sandwich-type $B_{12}\text{Cr}$ (C_{3v} , **9**) in Figure 2 and, with one more B_{12} ligand added along the three-fold molecular axis from the opposite side, the staggered 18-

Table 1. Optimized Bond Lengths (r), Calculated Natural Charges of Li Atoms (q_A), Lowest Vibrational Frequencies (ν_{min}), Total Wiberg Bond Indices of B Atoms (WBI_B), the Bond Orders of Interligand B–B' Interactions ($\text{WBI}_{B-B'}$), HOMO Energies, and NICS(1) Values 1.0 \AA Above the B_7 -Ring Centers of Some High Symmetry Tire-Shaped Structures at B3LYP/6-311+G(3df).

	Symmetry	r_{B-B} (\AA)	$r_{B-B'}$ (\AA)	r_{M-B} (\AA)	r_{A-M} (\AA)	q_A (lel)	ν_{min} (cm^{-1})	WBI_B	$\text{WBI}_{B-B'}$	HOMO (eV)	NICS(1) (ppm)
$B_{14}\text{Mn}^-$ (T)	D_{7d}	1.646	1.783	2.053			316	3.63	0.51	−1.32	−36
$\text{Li}B_{14}\text{Mn}$	C_{7v}	1.674, 1.618	1.764	2.114, 2.007	2.456	+0.90	307	3.68–3.74	0.52	−6.01	
$B_{14}\text{Fe}$ (T)	D_{7d}	1.643	1.771	2.048			313	3.60	0.54	−5.54	−38
$B_{14}\text{Fe}$	C_{7v}	1.614, 1.669	1.752	2.120, 1.992			286	3.61–3.68	0.57	−6.38	−28
$B_{14}\text{Fe}^-$ (D)	C_{7v}	1.628, 1.629	1.833	2.046, 2.047			269	3.63–3.70	0.46	−1.48	−33
$B_{14}\text{Co}^+$	C_{7v}	1.674, 1.633	1.730	2.005, 2.112			245	3.63–3.64	0.63	−11.39	−28
$(B_7)_2\text{Cr}^{2-}$	D_{7d}	1.643	1.847	2.064			199	3.72	0.43	+2.44	−24
$\text{Li} B_{14}\text{Cr}^-$	C_{7v}	1.677, 1.622	1.804	2.105, 2.030	2.425	+0.87	300	3.63–3.76	0.46	−1.63	
$\text{Li}_2 B_{14}\text{Cr}$	D_{7d}	1.646	1.815	2.060	2.487	+0.95	147	3.67	0.43	−5.27	

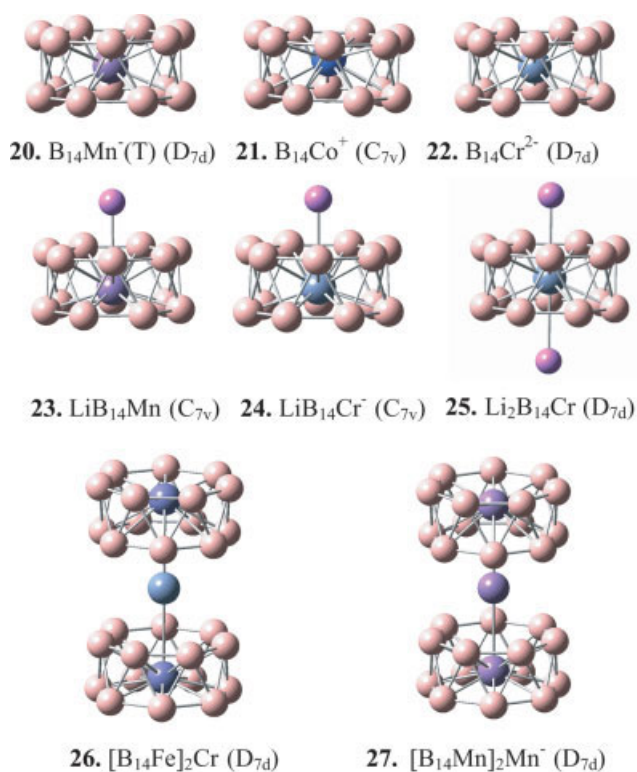


Figure 5. $B_{14}M$ molecular tires and their Li^+ -containing complexes at B3LYP/6-311+G(3df) and the double-tire sandwich-type $(B_{14}M)_2M^-$ complexes at B3LYP/6-31 + G(d)/Lanl2dz.

electron full sandwich-type $(B_{12})_2Cr$ (D_{3d} , **10**) is produced. Cr centers in both **9** and **10** can be replaced with all the transition metals in groups VB–VIIB of the periodic table to form 12-electron $B_{12}M$ and 18-electron $(B_{12})_2M$ complex series, respectively. In these complexes, B_{12} units serve as effective inorganic ligands, similar to the well-known organic ligands of C_6H_6 in $(C_6H_6)_2Cr$ and $C_5H_5^-$ in $(C_5H_5)_2Fe$. The lowest vibrational frequencies of the full sandwich-type $(B_{12})_2M$ complexes correspond to a rotary vibrational mode (a_{2u}) of the two B_{12} ligands about the three-fold molecular axis, similar again to the lowest-energy vibrational modes of $(C_5H_5)_2Fe$ and $(C_6H_6)_2Cr$. Bowl-shaped structures have also been obtained for 14-electron $B_{11}Co$ (C_1 , **4**), 16-electron $B_{13}Co$ (C_{2v} , **6**), and 16-electron $B_{14}Mn^-$ (C_2 , **7**) and $B_{14}Fe$ (C_2 , **15** and **17**), which are all confirmed to be true minima on their potential energy surfaces. Both singlet and triplet bowl-shaped $B_{14}Fe$ (C_2) were confirmed to be transition states with one imaginary vibrational frequency. They were automatically converted to more stable structures with lower symmetries (C_2 , structures **15** and **17**) when relaxed in the imaginary vibrational modes of the corresponding transition states. Stable bowl-shaped C_2 structures exist for $B_{14}Ru$, $B_{14}Os$, and other second- and third-row transition metal $B_{14}M$ complexes with the same number of valence electrons. NBO analyses indicate that, different from the $Li^+ - B_8^{2-}$ ionic interaction in LiB_8^- (C_{7v}),² effective π -d coordination bonds have been formed in these bowl-shaped complexes between the partially filled d valence orbitals of the transition metal M and the distorted delocalized π orbitals of the B_n ligands (see detailed MO pictures of $B_{12}Cr$ and $(B_{12})_2Cr$ in Supporting Information). Calculated Wiberg bond indices (WBIs) help to semi-quantitatively evaluate

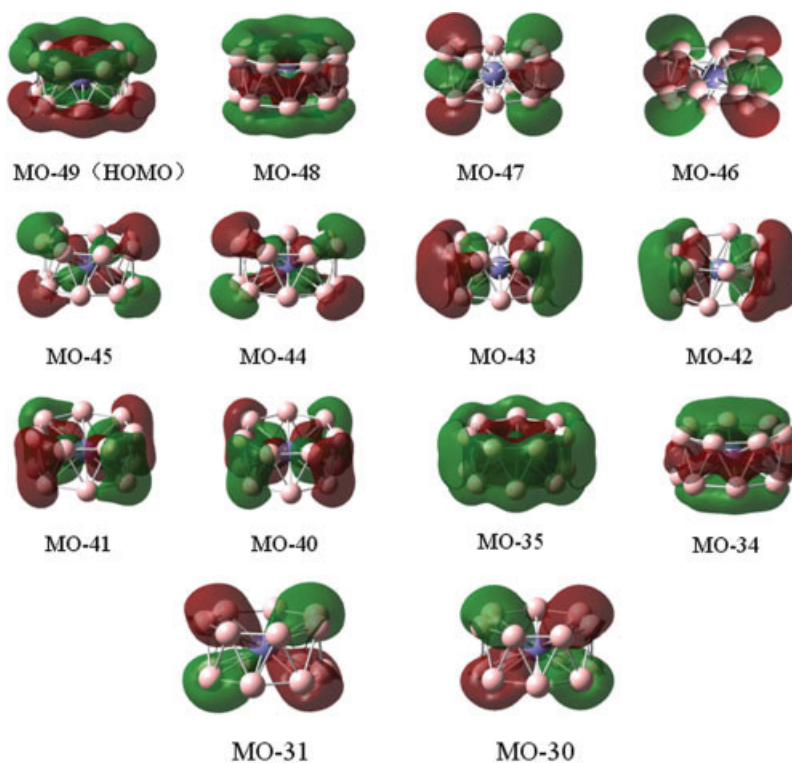


Figure 6. Some of the MO pictures of doublet $B_{14}Fe^-$ (C_{7v} , 18) involving the partially filled Fe 3d orbitals and the inter-ligand interactions which do not exist in normal sandwich-type complexes.

the overall π -d bonding effects in these complexes. For instances, the Co centers in B_8Co^+ (C_{7v}), $B_{10}Co^-$ (C_s), and $B_{12}Co^-$ (C_{3v}) possess the total bond orders of $WBI_{Co} = 2.71, 2.71,$ and $2.55,$ respectively.

Concerning the relative stabilities of the low-lying isomers of these systems, Figure 3a clearly indicates that, with zero-point energy (ZPE) corrections included, the bowl-shaped C_{3v} structure (**11**) is the ground-state of $B_{12}Co^-$: it lies 5.546 eV lower than the tire-shaped $B_{12}Co^-$ (**12**) and 5.489 eV lower than the face-capped icosahedral $B_{12}Co^-$ (**13**). The molecular bowls depicted in Figures 1–3 can be systematically obtained by coordinating a transition metal atom M from one side along the molecular axis of the lowest-lying planar or quasi-planar B_n neutrals or monoanions with 6 or 8 π electrons ($n = 8–14$).⁷ The 12-electron $B_{12}Cr$ (C_{3v}), 18-electron $(B_{12})_2Cr$ (D_{3d}), and 16-electron $B_{14}Fe$ (C_2) are the most interesting prototypes of bowl-shaped B_nM complexes to be targeted in future experiments. The formation energy of $B_{12}Cr$ with respect to free B_{12} and Cr in the process of $B_{12}(C_{3v}) + Cr \rightarrow B_{12}Cr(C_{3v})$ turns out to be $\Delta E_f = -169$ kJ/mol, while the corresponding value of $(B_{12})_2Cr$ with respect to $2B_{12}(C_{3v}) + Cr = (B_{12})_2Cr(D_{3d})$ is approximately doubled ($\Delta E_f = -328$ kJ/mol). For reactions $B_{10}(C_{2h}) + Ni = B_{10}Ni(C_s)$ and $B_{12}(C_{3v}) + Ni = B_{12}Ni(C_{3v})$, the calculated energy changes are $\Delta E_f = -214$ and -243 kJ/mol, respectively. These negative energy changes indicate that the formations of bowl-shaped B_nM complexes are favored in thermodynamics in gaseous phases over the corresponding systems of free transition metal M plus bare B_n ligands. DFT evidences obtained here strongly suggest that bowl-shaped fullerene analogues of B_n units (like the well-known bowl-shaped C_{20} ¹⁸) exist in small B_nM complexes with M including all the VB–VIII B transition metal elements in the periodic table. As a robust structural unit with the right curvature, C_{3v} , B_{12} ⁸ is also expected to serve as strong molecular caps (or covers) to seal open tubular boron clusters^{8,19} with suitable diameters to form closed or half closed B_n tubes.

$B_{14}M$ Molecular Tires ($M = Mn, Fe, Co$)

Although B_nM favor bowl-shaped structures when $n < 14$, the stabilities of tire-shaped B_nM complexes ($M = Mn, Fe, Co$) catch up with their bowl-shaped isomers when the sizes of the ligands reach $n = 14$ and, in the cases of $B_{14}Fe^-$ monoanion and $B_{14}Co^+$ monocation, the former structures become clearly more stable than the latter. For $B_{14}Fe$ neutrals, the initially constructed normal sandwich-type geometry collapsed unexpectedly into a D_{7d} molecular tire during structural optimization and the triplet tire-shaped D_{7d} structure (**14**) turned out to have the lowest energy in its low-lying isomers: it lies 0.052 eV lower than triplet $B_{14}Fe$ (C_2 , **15**), 0.146 eV lower than singlet $B_{14}Fe$ (C_{7v} , **16**), and 0.575 eV lower than the singlet $B_{14}Fe$ (C_2 , **17**) in energies. With ZPE corrections included, the corresponding energy differences are slightly changed to $-0.059, +0.166,$ and $+0.469$ eV, respectively (see Fig. 3b). Given the accuracy of the DFT method used in this work and the small energy differences obtained, the first three isomers of $B_{14}Fe$ (**14**, **15**, and **16**) should be considered isoenergetic in thermodynamics and they would co-exist in experiments. To further study the properties of $B_{14}Fe$

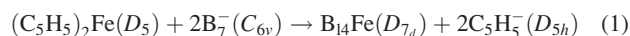
system, we check the behavior of $B_{14}Fe^-$ monoanions. With one extra electron added to a neutral $B_{14}Fe$ (C_{7v}), a doublet $B_{14}Fe^-$ (C_{7v} , **18**) is produced with the Fe center located only 0.05 Å above the tubular center of the system along the seven-fold molecular axis. As indicated in Figure 3c, with ZPE correction included, the tire-shaped $B_{14}Fe^-$ (**18**) lies 0.688 eV lower than its bowl-shaped C_2 isomer (**19**) (the corresponding energy difference is increased to 0.777 eV without ZPE correction). This energy difference is significant, indicating that the tire-shaped $B_{14}Fe^-$ monoanion (**18**) is overwhelmingly favored in thermodynamics over its bowl-shaped isomer (**19**). It would be highly populated in equilibrium states and, therefore, be detectable in experiments. The energy difference between the anion and the neutral at the anion structure defines the first vertical detachment energy (VDE) of the anion and relaxing the neutral to its ground-state gives rise to the electron affinity of the neutral (EA).⁸ As $B_{14}Fe^-$ (**18**) is clearly the lowest-lying structure of the monoanion while triplet $B_{14}Fe$ (**14**) and singlet $B_{14}Fe$ (**16**) lie very close in energies, two sets of one-electron detachment energies are predicted by DFT, with $VDE(D \rightarrow T) = 3.03$ eV, $EA(D \rightarrow T) = 2.87$ eV and $VDE(D \rightarrow S) = 4.00$ eV, $EA(D \rightarrow S) = 3.02$ eV, respectively. Future measured VDE and EA values will help to determine the ground-state structure of $B_{14}Fe$ neutral in its low-lying isomers (**14–17**).

The calculated IR spectra of tire-shaped D_{7d} $B_{14}Fe$ (**14**) and C_{7v} $B_{14}Fe$ (**16**) neutrals in Figure 4 appear to be quite similar in general shapes with the main absorption peaks located between 515 and 545 cm^{-1} , while the strongest absorption of the tire-shaped $B_{14}Fe^-$ monoanion (C_{7v} , **18**) is moved to a lower frequency at 422 cm^{-1} (see Fig. 4). The IR spectra of these high-symmetry tire-shaped complexes are relatively simple. However, the IR spectrum of bowl-shaped $B_{14}Fe$ (C_2 , **15**) becomes much more complicated with the main peak located at 1457 cm^{-1} and many weaker absorptions at lower frequencies, providing clear theoretical evidences to characterize this bowl-shaped structure from its tire-shaped isomers in future spectroscopic investigations.

Similar to $B_{14}Fe$, a triplet $B_{14}Mn^-$ (D_{7d} , **20**) is almost isoenergetic with its triplet C_2 isomer and it can be further stabilized by the introduction of a Li^+ counterion to form a singlet $LiB_{14}Mn$ (C_{7v} , **23**). For $B_{14}Co^+$ monocation, the lowest-lying state takes a singlet tire-shaped C_{7v} structure (**21**) which lies 0.631 eV lower than its triplet D_{7d} isomer and 0.502 eV lower than the bowl-shaped triplet C_2 structure. The DFT evidences obtained above strongly suggest that the bowl-to-tire structural transition occurs to the first-row transition metal complexes B_nM ($M = Mn, Fe, Co$) at $n = 14$, where, as a result of the increased stresses caused by the high curvatures of the distorted B_{14} in bowl-shaped $B_{14}M$, the quasi-planar B_{14} units have been rearranged into tubular conformations (D_{7d} or C_{7v}) to better coordinate the transition metal center M by surrounding it in the more stable tire-shaped isomers. The singlet $B_{14}Cr^{2-}$ dianion (D_{7d} , **22**), which possesses a positive highest occupied MO (HOMO) energy, can be effectively stabilized by introducing Li^+ counterion(s) into the system to form a C_{7v} $LiB_{14}Cr^-$ monoanion (**24**) or a $Li_2B_{14}Cr$ neutral (D_{7d} , **25**), which all turned out to possess negative HOMO energies and be true minima on their potential energy surfaces (see Table 1). The calculated formation energies of neutral $B_{14}Fe$ (**14**), $LiB_{14}Mn$ (**23**), and $Li_2B_{14}Cr$ (**25**) with

respect to free component atoms in gaseous phases are -6671 , -7114 , and -7747 kJ/mol, respectively. These huge negative formation energies support the tire-shaped structures proposed in this work. Singlet $B_{14}M$ (C_{7v}) complexes with $M = Ru, Rh, Os, Re,$ or Ir have also been confirmed to be true minima. But these tire-shaped heavy transition metal complexes are clearly less stable than their bowl-shaped C_2 isomers, possibly due to the fact that heavy transition metals are too big in size to be hosted at the centers of tubular B_{14} ligands. The tire-shaped $B_{14}M$ complexes ($M = Cr, Mn, Fe, Co$) obtained in this work with the approximate diameters of 3.8 \AA contain the thinnest tubular B_n units obtained so far in small B_n series.^{8,19} We conclude that the introduction of the first-row transition metal centers M helps to stabilize the tubular B_n structural units at $n = 14$, a size clearly smaller than $n = 20$ where the 2D-3D structural transition occurs to bare B_n clusters.⁸ In other words, a tubular B_{14} (D_{7d}) with two degenerate imaginary frequencies at 400 cm^{-1} can be effectively stabilized in its tire-shaped first-row transition metal complexes $B_{14}M$ ($M = Mn, Fe, Co$). With a bigger tubular ligand of B_{16} (which is a true minimum at D_{8d} symmetry with the lowest vibrational frequency of 180 cm^{-1}), the tire-shaped $B_{16}Ti^{2-}$ (D_{8d}) and the slightly distorted $LiB_{16}Ti^-$ (C_3) all turned out to be true minima on their potential energy surfaces.

Neutral $B_{14}Fe^{14}$, which possesses the lowest vibrational frequency of 313 cm^{-1} , is particularly interesting. A 6π -electron B_7^- (D_{7h}) monoanion in $B_{14}Fe$ behaves similar to the well-known $C_5H_5^-$ ligand (D_{5h}) in ferrocene (though the interligand distance has been severely depressed in $B_{14}Fe$). It would be intriguing to study the following ligand-exchange reaction from ferrocene (C_5H_5)₂Fe to $B_{14}Fe$:



with ZPE corrections included, eq. (1) is favored in thermodynamics at DFT level: it has the total energy change of $\Delta E^\circ = -262$ kJ/mol, enthalpy change of $\Delta H^\circ = -266$ kJ/mol, and Gibbs free energy change of $\Delta G^\circ = -245$ kJ/mol. Replacing $B_{14}Fe$ (D_{7d} , **14**) in eq. (1) with its isomers $B_{14}Fe$ (C_{2v} , **15**) or $B_{14}Fe$ (C_{7v} , **16**) only slightly changes these calculated thermodynamic quantities (about 16 kJ/mol) for the reason that structures **14**, **15**, and **16** are almost isoenergetic as detailed above. As B_7^- has been observed in gaseous phases,³ eq. (1) may be a viable route to synthesize neutral $B_{14}Fe$ and/or a mixed sandwich-type $(B_7)Fe(C_5H_5)$ intermediate by trapping B_7^- anions with ferrocene.

Orbital Analyses

The high stabilities of the tire-shaped structures stem from their special bonding patterns. Tire-shaped $B_{14}Mn^-$, $B_{14}Fe$, $B_{14}Co^+$, and $B_{14}Cr^{2-}$ all conform to the 18-electron requirement. Each B_7^- (D_{7h}) ligand provides three occupied π MOs to interact with the partially filled 3d orbitals of the transition metal center M . The first-row transition metal centers fit well with the tubular B_{14} ligands in these complexes, both geometrically and electronically. Of the MO pictures of $B_{14}Fe^-$ (see Fig. 6), the degenerate MO-45, MO-44, MO-31, and MO-30 involve Fe $3d_{xz}$ and $3d_{yz}$; MO-41 and MO-40 consist of contributions from Fe $3d_{xy}$

and $3d_{x^2-y^2}$, and Fe $3d_{z^2}$ mainly participates in the formations of MO-48, MO-35, and MO-34. In addition to the 14 M-B coordination interactions between the M center and the two parallel B_7 ligands (“the spokes of the tires”), these severely depressed tire-shaped complexes along the seven-fold molecular axes possess short enough B-B' distances to form 14 effective interligand interactions between neighboring B atoms in different B_7 ligands (“the rims of the tires”). MO-48–MO-46, MO-43–MO-40, MO-35, and MO-34 of $B_{14}Fe^-$ all involve such interligand interactions. These interligand B-B' interactions have the approximate total Wiberg bond indices of $WBI_{B-B'} \approx 0.5$ (see Table 1), while the bond orders of the intraligand B-B interactions along the peripheries of the B_7 rings are close to $WBI_{B-B} \approx 1.0$. It is obvious that, in addition to the B-M coordination interactions, each B atom in these complexes forms two single B–B bonds with two neighboring B atoms in the B_7 ligand it belongs to and two “half” B–B' bonds with two neighboring B atoms in the opposite B_7 ligand. It was the formations of these interligand interactions that made the initial normal sandwich-type $(B_7)_2M$ geometries ($M = Mn, Fe, Co$) collapse automatically into the severely depressed tire-shaped structures during optimizations. The bonding patterns in these depressed molecular tires are obviously different from the situation in normal sandwich-type complexes (like $(C_5H_5)_2Fe$ and $(B_nX)_2M^{12}$), in which the two ligands are separated by the central atom and there exist no direct interactions between atoms in different ligands. The high total bond orders of B atoms with $WBI_B = 3.61 - 3.76$ (see Table 1) support the bonding patterns in these tire-shaped structures. The overall bonding effects discussed above overcomes the stress in tire-shaped $B_{14}M$ and makes them more stable than their more open bowl-shaped isomers.

NBO analyses indicate that the valence MOs of tire-shaped $B_{14}M$ can be clearly traced back to various combinations of the valence MOs of the two B_7^- ligands and the partially filled 3d orbitals of transition metal atom M . For examples, the degenerate MO-47 and MO-46 of $B_{14}Fe^-$ (see Fig. 6) mainly represent the in-phase overlaps of the degenerate π -HOMOs of the two B_7^- ligands in vertical directions; MO-48 and MO-34 involve the out-of-phase and in-phase overlaps between the totally delocalized π -orbitals (HOMO-2) of B_7^- ligands and $3d_{z^2}$ orbital of Fe center, and the HOMO (MO-49) of $B_{14}Fe^-$ basically consists of the contribution from the delocalized σ orbital (HOMO-1) of the B_7^- ligands. In fact, both the delocalized π orbitals perpendicular to the B_7 planes and delocalized σ orbitals along the peripheries of the B_7 rings have been basically kept in $B_{14}M$ complexes with more or less distortions. The calculated HOMO-LUMO energy difference of 2.83 eV obtained for $B_{14}Fe^-$ represents the typical HOMO-LOMO gap values of the B_nM series. The negative NICS(1) values tabulated in Table 1 confirm the existence of ring current effects above B_7^- ligands in $B_{14}M$ series (compare with the corresponding NICS(1) values of -23 ppm obtained for free B_7^- (D_{7h}) at the same theoretical level). $B_{14}M$ complexes possess higher negative NICS(1) values than free B_7^- ligand mainly because of the influences of the $3d_{z^2}$ orbitals of transition metal centers which are located about 1.85 \AA below the ghost atoms along the seven-fold molecular axes. The HOMO-LUMO energy gaps of these molecular bowls and tires are confirmed to be greater than 2.4 eV.

$[B_{14}M]_2M'$ Double Molecular Tires

Two tire-shaped $B_{14}M$ units discussed above can be further utilized as ligands to coordinate another transition metal M' to form a double-tire sandwich-type $[B_{14}M]_2M'$ complex, as shown in the cases of $[B_{14}Fe]_2Cr$ (D_{7d} , **26**) and $[B_{14}Mn]_2Mn^-$ (D_{7d} , **27**) in Figure 5. All the transition metal centers M and M' in these structures satisfy the 18-electron requirement. These staggered structures contain an $M-M'-M$ chain composed of three transition metal atoms along the seven-fold molecular axis. They are confirmed to be true minima on their potential energy surfaces and the rotary energy barriers from the staggered to the eclipsed isomers (which are transition states) turn out to be close to 2 kcal/mol. These energy barriers could be significantly increased by substituting B atom(s) with other group(s) (like CH) to develop molecular motors similar to metallacarboranes.²⁰

Supporting Information

Optimized coordinates, total energies, and the lowest vibrational frequencies of 106 B_nM complexes (compared with tubular B_{14} and B_{16}) and the calculated infrared (IR) spectra and MO pictures of some prototypic complexes are available from <http://www.xztc.edu.cn/lisidian> and the corresponding author.

Summary

In conclusion, we have presented in this work a new class of bowl- and tire-shaped transition metal–boron complexes B_nM and double-tire sandwich-type complexes $[B_nM]_2M'$ at DFT level. Small B_n clusters prove to be effective inorganic ligands to coordinate a wide range of transition metal atoms and the introduction of the first-row transition metal centers helps to stabilize the tire-shaped B_nM structures ($M = Mn, Fe, Co$) in a size range starting at $n = 14$. These B_nM complex bowls and tires with transition metal centers possess novel geometrical structures and bonding patterns different from both the half-sandwich-type $B_nA^{2,10,11}$ and H saturated molecular wheels of $C_2B_{12}H_{12}$ and $C_2B_{10}H_{10}$.²¹ The B_nM complex series proposed in this work are expected to be synthesized in gaseous phases in future experiments to open a new branch of chemistry on transition metal–boron complexes.

References

- Zhai, H.-J.; Alexandrova, A. N.; Birch, K. A.; Boldyrev, A. I.; Wang, L.-S. *Angew Chem Int Ed* 2003, 42, 6004.
- Alexandrova, A. N.; Zhai, H.-J.; Wang, L.-S.; Boldyrev, A. I. *Inorg Chem* 2004, 43, 3552.
- Alexandrova, A. N.; Boldyrev, A. I.; Zhai, H.-J.; Wang, L.-S. *J Phys Chem A* 2004, 108, 3509.
- Alexandrova, A. N.; Boldyrev, A. I.; Zhai, H.-J.; Wang, L.-S.; Steiner, A.; Fowler, P. W. *J Phys Chem A* 2003, 107, 1359.
- Zhai, H.-J.; Wang, L.-S.; Alexandrova, A. N.; Boldyrev, A. I. *J Chem Phys* 2002, 117, 7917.
- Zhai, H.-J.; Wang, L.-S.; Alexandrova, A. N.; Boldyrev, A. I.; Zakrzewski, V. G. *J Phys Chem A* 2003, 107, 9319.
- Zhai, H.-J.; Kiran, B.; Li, J.; Wang, L.-S. *Nat Mater* 2003, 2, 827.
- Kiran, B.; Bulusu, S.; Zhai, H.-J.; Yoo, S.; Zeng, X. C.; Wang, L.-S. *Proc Natl Acad Sci* 2005, 102, 961.
- Aihara, J.-I.; Kanno, H.; Ishida, T. *J Am Chem Soc* 2005, 127, 13324.
- Li, Q.-S.; Jin, Q. *J Phys Chem A* 2003, 107, 7869.
- Li, Q.-S.; Gong, L.-F. *J Phys Chem A* 2004, 108, 4322.
- Li, S.-D.; Guo, J.-C.; Miao, C.-Q.; Ren, G.-M. *Angew Chem Int Ed* 2005, 44, 2158.
- Exner, K.; Schleyer, P. V. R. *Science* 2000, 290, 1937.
- (a) Becke, A. D. *J Chem Phys* 1993, 98, 5648; (b) Miehlich, B.; Savin, A.; Stoll, H.; Preuss, H. *Chem Phys Lett* 1989, 157, 200.
- (a) Hay, P. J.; Wadt, W. R. *J Chem Phys* 1985, 82, 299; (b) Hay, P. J.; Wadt, W. R. *J Chem Phys* 1985, 82, 270.
- Schleyer, P. V. R.; Maerker, C.; Dransfeld, A.; Jiao, H. J.; Hommes, N. *J Am Chem Soc* 1996, 118, 6317.
- Frisch, M. J.; Trucks, G. W.; Schlegel, H. B.; Scuseria, G. E.; Robb, M. A.; Cheeseman, J. R.; Montgomery, J. A., Jr.; Vreven, T.; Kudin, K. N.; Burant, J. C.; Millam, J. M.; Iyengar, S. S.; Tomasi, J.; Barone, V.; Mennucci, B.; Cossi, M.; Scalmani, G.; Rega, N.; Petersson, G. A.; Nakatsuji, H.; Hada, M.; Ehara, M.; Toyota, K.; Fukuda, R.; Hasegawa, J.; Ishida, M.; Nakajima, T.; Honda, Y.; Kitao, O.; Nakai, H.; Klene, M.; Li, X.; Knox, J. E.; Hratchian, H. P.; Cross, J. B.; Adamo, C.; Jaramillo, J.; Gomperts, R.; Stratmann, R. E.; Yazyev, O.; Austin, A. J.; Cammi, R.; Pomelli, C.; Ochterski, J. W.; Ayala, P. Y.; Morokuma, K.; Voth, G. A.; Salvador, P.; Dannenberg, J. J.; Zakrzewski, V. G.; Dapprich, S.; Daniels, A. D.; Strain, M. C.; Farkas, O.; Malick, D. K.; Rabuck, A. D.; Raghavachari, K.; Foresman, J. B.; Ortiz, J. V.; Cui, Q.; Baboul, A. G.; Clifford, S.; Cioslowski, J.; Stefanov, B. B.; Liu, G.; Liashenko, A.; Piskorz, P.; Komaromi, I.; Martin, R. L.; Fox, D. J.; Keith, T.; Al-Laham, M. A.; Peng, C. Y.; Nanayakkara, A.; Challacombe, M.; Gill, P. M. W.; Johnson, B.; Chen, W.; Wong, M. W.; Gonzalez, C.; Pople, J. A. *Gaussian 03, Revision A.1*, Gaussian, Inc., Pittsburgh, PA, 2003.
- Prinzbach, H.; Weiler, A.; Landenberger, P.; Wahl, F.; Worth, J.; Scott, L. T.; Gelmont, M.; Olevano, D.; Issendorff, B. V. *Nature* 2000, 407, 60.
- Boustani, I.; Quandt, A. *Europhys Lett* 1997, 39, 527.
- Hawthorne, M. F.; Zink, J. I.; Skelton, J. M.; Bayer, M. J.; Liu, C.; Livshits, E.; Baer, R.; Neuhauser, D. *Science* 2004, 303, 1849.
- Wang, Z.-X.; Schleyer, P. V. R. *Angew Chem Int Ed* 2002, 41, 4082.